The dynamic mode of high-resolution cathodoluminescence microscopy

2004 J. Phys.: Condens. Matter 16 S75

(http://iopscience.iop.org/0953-8984/16/2/009)

INSTITUTE OF PHYSICS PUBLISHING JOURNAL OF PHYSICS: CONDENSED MATTER

J. Phys.: Condens. Matter **16** (2004) S75–S84 PII: S0953-8984(04)68633-4

The dynamic mode of high-resolution cathodoluminescence microscopy

J Schreiber and S Vasnyov

Martin-Luther-Universitaet, Fachbereich Physik, Friedemann-Bach-Platz 6, D-06108 Halle/Saale, Germany

E-mail: schreiber@physik.uni-halle.de

Received 5 September 2003
Published 22 December 2003
Online at stacks.iop.org/JPhysCM/16/S75 (DOI: 10.1088/0953-8984/16/2/009)

Abstract

The dynamic mode of scanning electron microscopy (SEM) cathodoluminescence (CL) based on computer-aided acquisition and fast processing of image data is introduced as a unique method to reveal glide dislocations as extended mobile recombination centres in several III/V and II/VI semiconductors with zincblende and wurtzite lattice structure respectively. Local plastic deformation by *in situ* scratching or indentation at low-index sample surfaces is shown to be easily used to generate and propagate individual single dislocations of various types. Dislocation dynamics and defect-related recombination activity, as simultaneously observed at separate moving dislocation segments having screw- or edge-type structure, are considered by analysing the CL movies taken.

Our results give evidence of a complex relationship between dynamic and recombination active defect properties depending on the structure of the dislocation and the material studied. In particular, polar A(g) and B(g) dislocations are clearly different in respect of both their dynamics and recombination active behaviour, as discussed for fresh glide dislocations in ZnO and GaAs samples.

1. Introduction

The dynamic mode of cathodoluminescence (CL) microscopy, referred to as 'Dyn CL' in the following, is an advanced experimental method for use with scanning electron microscopy (SEM) employing the technique of kinematic imaging, so far rarely used in the field of SEM [1]. Dyn CL will be introduced as a powerful tool which provides essential information on radiative or non-radiative carrier recombination effects at individual single dislocations being generated and propagated in semiconductor crystals. Dislocation-induced recombination is reflected by defect-bound microscopic CL contrast patterns formed along the defect lines depending on the distinct structure of the local dislocation segment [2]. Dyn CL is shown to be an appropriate procedure for revealing dislocations as extended mobile recombination centres [3]. The Dyn CL studies carried out under high-resolution conditions comprise observation of dislocation dynamics on a microscopic scale, such as glide motion in various slip systems or defect reactions, as well as an analysis of the CL contrast behaviour at both moving and resting dislocations [4]. Such types of experiment aim at the disclosure of a possible correlation between the dynamics and recombination behaviour observed at an identical defect segment.

Furthermore, dislocation type-dependent recombination activity is generally expected to occur in the crystalline semiconductors. Corresponding differences in the particular defect-related CL contrasts may appear for two reasons; first of all, due to a distinct defect structure for screw- and edge-type dislocations including polar core configurations [5, 6], and secondly, because of structural alterations when an identical dislocation segment turns from a dynamical into a stationary state [7]. The latter may be regarded as a real dynamics-related impact on the recombination activity of glide dislocations.

For instance, in CdTe and ZnSe polar B(g) dislocation segments have been identified as radiative recombination centres emitting so-called ‘Y luminescence’ [6, 8]. But, on the other hand, activity as an extended non-radiative recombination centre appears to be a common property of most types of dislocation in various semiconductors. Differences in the strength of non-radiative recombination relating to distinct types of dislocation have not been proved until now.

This paper presents the results of very recent experimental work performed using Dyn CL for *in situ* studies on plastic microdeformation resulting in the generation and thermally activated propagation of isolated single glide dislocations, and also by using Dyn CL for the observation of REDG (recombination enhanced dislocation glide) effects [9] in ZnO and GaAs samples. Microdeformation experiments by means of scratching or indentation on low-index sample surfaces *in situ* demonstrate the introduction of fresh dislocations and the formation of regular microscopic defect configurations in the crystalline samples. Taking advantage of the simultaneous operation of several slip systems, dislocations of various types are shown to be produced; in this way, defect configurations with recognizable screw- and edge-type dislocation segments are available. In particular, polar A(g) and B(g) edge-type dislocation parts such as occur in the main slip systems of the zincblende [10] and wurtzite [11] lattice structures can be verified in the GaAs and ZnO samples respectively.

For the first time, detailed considerations of dislocation dynamics on a microscopic scale in correlation with the CL contrast behaviour on individual moving dislocation segments are reported. The CL contrast recorded at a dislocation during slip motion proves directly the intrinsic origin of dislocation recombination activity.

As shown in [4], CL contrast measurements can be employed to establish a possible relationship between local slip velocity and momentary contrast value. Some effects of possible defect reactions are demonstrated.

2. Experimental details

The kinematic mode of SEM CL is realized by means of generating and storing image sequences with frame rates up to real-time imaging conditions. The Dyn CL technique can document a complete history of dislocation movement and corresponding CL defect contrast behaviour over a period of up to 1 h. An advanced digital scanning and signal acquisition system is available for real-time imaging and fast data processing. The frame rates used result from pixel acquisition times limited by a given signal-to-noise ratio, and depend on the frame size chosen. In order to save quantitative CL information over a dynamic range of 12 bit, the uncompressed AVI format must be exploited for movie storage. The Dyn CL mode is part of

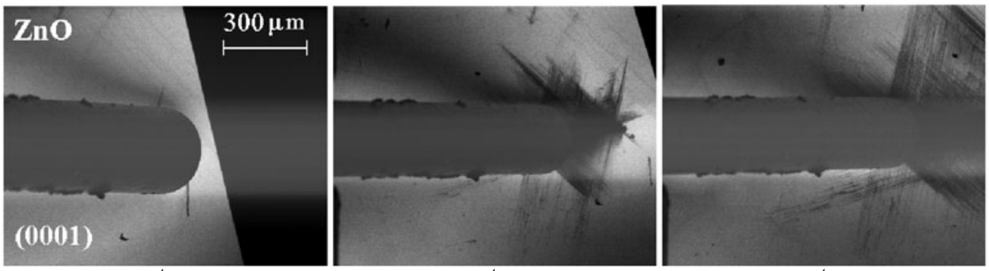

Figure 1. Employing Dyn CL for observation of local plastic deformation by *in situ* scratching on (0001) ZnO sample. Propagation of highly mobile dislocations in various prismatic slip systems at room temperature is seen. Order on timescale: $t_0 < t_n < t_x$.

a conventional SEM apparatus (JSM 6400, Jeol) equipped with a CL attachment (Mono CL, Oxford Instruments) and cooling stage (CF302, Oxford Instruments). Sequential CL imaging based on panchromatic signal acquisition with frame rates up to 10 frames per second according to a minimum pixel acquisition time of 0.4 μs for a frame size of 500 $\times$ 500 is performed by utilizing a new electronic system providing dynamical frame grabbing even under TV-like conditions (DISS 4, Point Electronic GmbH).

Sample materials studied are III/V and II/VI semiconductor bulk crystals with high-quality polished sample surfaces. GaAs and ZnO samples were chosen for their zincblende lattice and wurtzite structure, respectively.

For the purpose of *in situ* local plastic deformation a special microindentation set-up was developed and installed [12]. *In situ* treatment of the sample and correlated CL observation can be carried out at temperatures between 300 and 72 K. Optimized electron beam probe conditions (20 keV, 1 nA) are employed for high-resolution CL imaging and excitation of the REDG effect in GaAs [13] and ZnO [14].

3. Results

The Dyn CL mode has been employed to investigate simultaneously microscopic dynamics and recombination activity of glide dislocations moving in the zincblende or wurtzite crystal matrices of the GaAs and ZnO bulk samples.

The results presented in the following demonstrate 'low-temperature' plastic deformation carried by the primary slip systems operating in the materials investigated. Dislocation glide movement originating from the thermal Peierls mechanism and/or the REDG effect is proved in both materials between room temperature and 72 K.

First, dynamic SEM CL is described as applied to *in situ* studies of the microscopic plastic deformation in ZnO. These experiments deal with examination of the intrinsic recombination properties of freshly produced glide dislocations. Figure 1 illustrates the observation of local plastic deformation during *in situ* scratching on the (0001) surface of the ZnO sample.

The dislocation arrangement generated is pictured by the defect-related CL dark contrasts. Distribution of the defect contrasts reveals typical slip systems as activated in the near-surface region. The process of local plastic deformation appears to be dominated by the prismatic slip $\{10\bar{1}0\}\langle\bar{1}2\bar{1}0\rangle$ systems producing highly mobile glide dislocations having a-type Burger's vectors. The ZnO bulk sample comes out as a relatively ductile material, evidenced by the observed propagation of dislocations over extremely large distances.

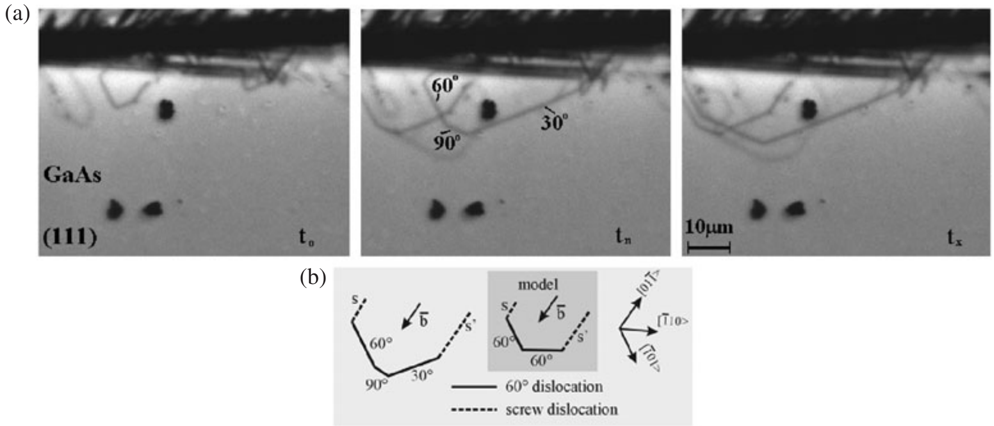

Figure 2. Identification by Dyn CL (a) of recombination active 30°, 60° and 90° edge-type line segments developing within dislocation half-loops, and schematic arrangement (b) of distinct dislocation segments in half-loop structure. Order on timescale: $t_0 < t_n < t_x$.

High-resolution scanning CL microscopy allows direct observation of individual single dislocations, providing a unique opportunity to consider explicitly any recombination-related effects depending on the structural type of particular dislocation segments. In surface-parallel dislocation-loop configurations certain basic types of glide dislocation structure formed in the zincblende or wurtzite crystals may be recognized. An illustrative example is given in figure 2. The series of CL images shows the formation of larger dislocation half-loops extending in surface-parallel glide planes of a (111) GaAs sample.

The defects propagate due to the REDG effect [13] in the GaAs sample. Based on scheme in figure 2 some 90°, 60°, 30° and screw-type line parts are identified. A closer look at the CL contrast features shows that there is no remarkable difference in the contrast strengths found at the distinct line segments. On the other hand, the mobility of the various line segments is seen to be clearly type-dependent.

The dynamic CL mode if utilized in high-resolution CL microscopy offers straightforward access to the dislocation dynamics on the microscopic scale of some tens of microns not covered by TEM or by x-ray topography or improved etching techniques. The SEM CL video movies verify thermally activated dislocation movement as well as operating the REDG effect at separate single defects under identical conditions.

The Dyn CL studies performed disclose interesting particularities of the microscopic dislocation dynamics. In figure 3 events of antiparallel slip and formation or back formation of dislocation parts in the common strain field are displayed.

The sequence of CL images in figure 3(a) displays the movement of single dislocations in opposite directions under the conditions of the same strain field. This antiparallel slip motion probably originates as a result of the different signs of the Burger's vectors belonging to the dislocations under consideration. Such a difference in the Burger's vectors might also explain the simultaneous occurrence of some processes of dislocation formation and back formation of dislocations in the same sample area. Figures 3(b) and (c) show the formation and back formation of surface-parallel line segments (s) accompanying threading dislocation segments (e) moving near a scratch placed on a (0001) or $(10\bar{1}0)$ surface of a ZnO sample. In the case of figure 3(a) the threading segment is pulling out a surface-parallel defect line which seemingly has a screw-type character. In the series of figure 3(c) the local dislocation configuration marked by (s) and (e) shrinks mainly due to disappearance of the surface-parallel

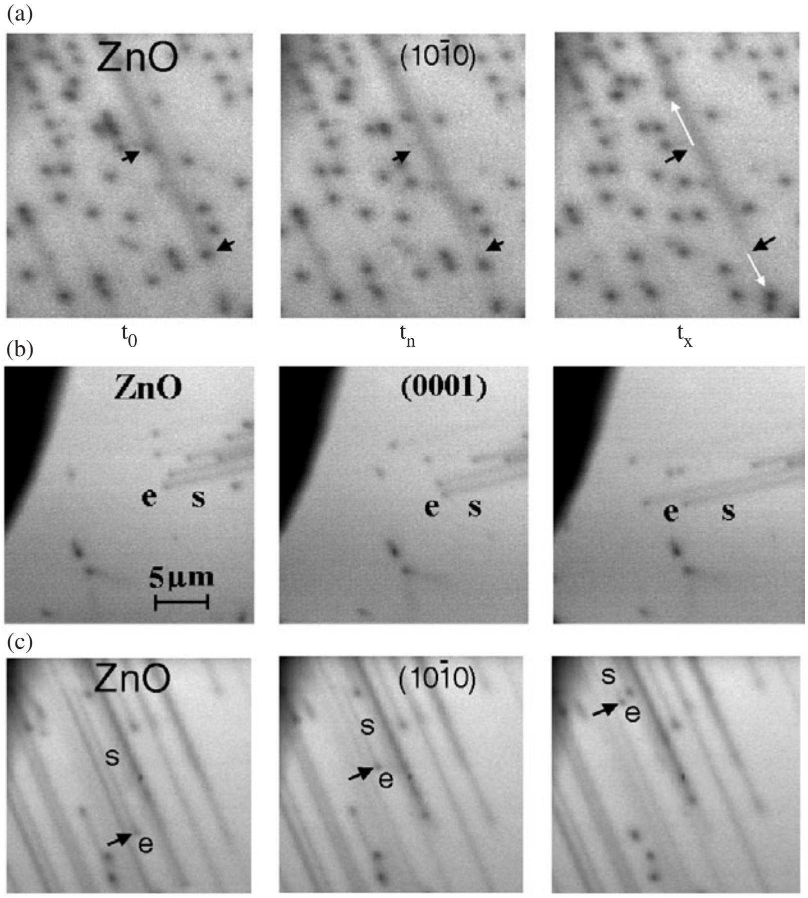

Figure 3. Microscopical dynamic behaviour of single dislocations as revealed by kinematic SEM CL. The series of CL images (a) illustrates antiparallel slip motion of threading dislocation segments observed on a (10$\bar{1}$0) ZnO sample. CL series (b) and (c) document the formation and back formation of surface-parallel screw-type defect line parts (s) accompanied with mobile threading dislocation segments (e). Lengths of line segments pulled out or removed are of the order of some micrometres. Order on timescale: $t_0 < t_n < t_x$.

screw line part (s) being found to be almost immobile. This defect reaction may be regarded as an elementary step in the recovery process if local stress is removed.

Figure 4 deals with the movement of two single threading dislocation segments (D, D*) slipping in closely neighbouring glide planes, driven by the same strain field gradient near the edge of a scratch on the (111)GaAs sample surface. The local situation is pictured in the CL micrograph of figure 4.

The so-called DCD (dynamic contrast diagram) plot [4] displayed in figure 4 has been derived from the corresponding CL movie. It shows accelerated and decelerated defect motion depending on the defect considered. Local velocity values are represented by the slope of the DCD patterns.

In figure 5 the glide movement of similar dislocation segments in a group of half-loops propagating in closely spaced (111) glide planes is studied. The chosen line segments D_1, D_2, D_3, D_4, probably the 60° parts of the half-loops, behave very similarly, as pointed out by the DCD plot which shows a decelerated motion for all of the segments measured. Figure 6

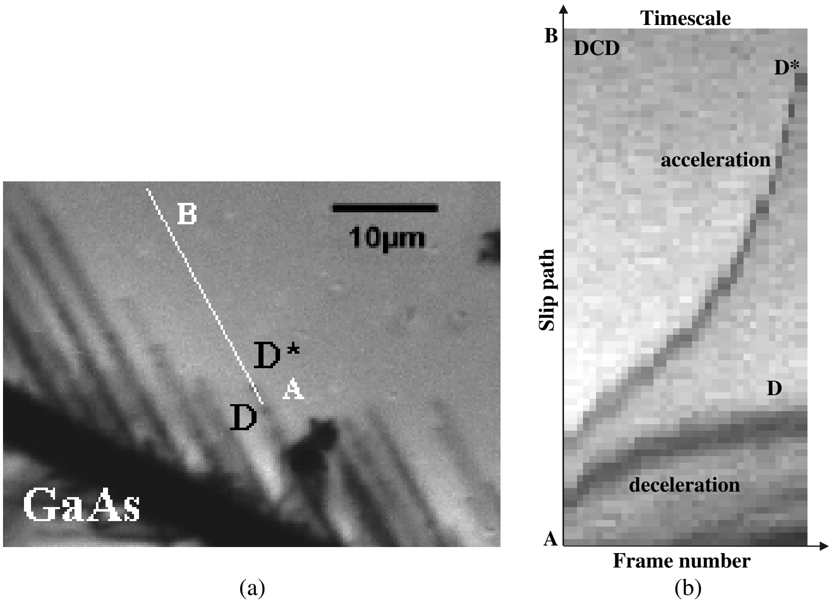

Figure 4. Dynamics of neighbouring single threading dislocations moving in a similar slip system of GaAs as illustrated in the CL micrograph (a). The DCD plot (b) proves acceleration for defect D* and deceleration for dislocation D. The entire timescale is 8 s.

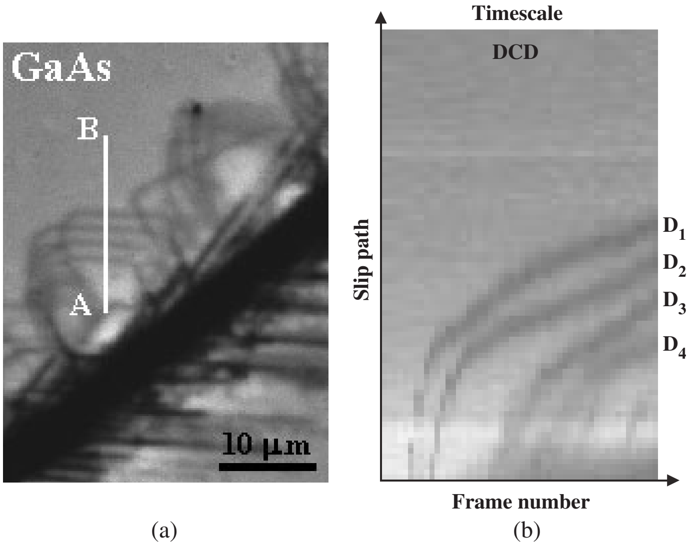

Figure 5. Movement of dislocation segments (D_1, D_2, D_3, D_4) of similar structural type in the group of half-loops is shown in a CL image (a). The half-loops expand in the (111) glide planes of GaAs. The DCD plot (b) shows patterns featuring decelerated motion for each of the segments included. The entire timescale is 10 s.

illustrates a study of the interaction of a resting defect (d) with a moving dislocation (e) as realized by the Dyn CL mode.

As the mobile dislocation segment approaches the sessile defect it therefore becomes pinned, and as a consequence of the interaction which occurs, a surface-parallel line defect

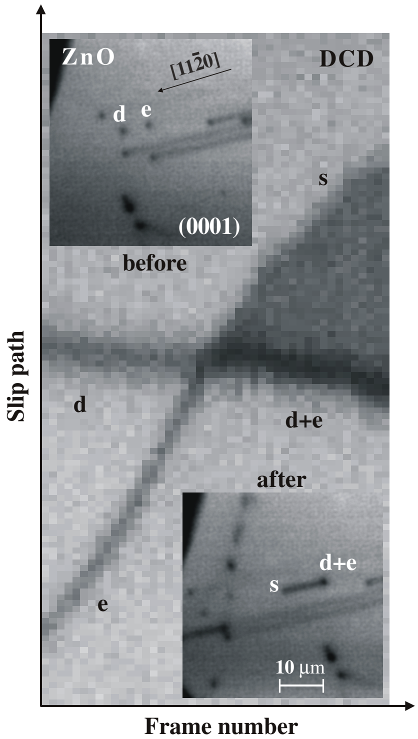

Figure 6. Dyn CL study of the interaction between resting defect (d) and the approaching slipping threading dislocation segment (e). The defect reaction observed is shown in the insets. Dynamics and contrast behaviour of individual defects (d, e, s) and defect complex (d + e) are represented by the DCD plot. (s) labels the screw-type line defect generated.

configuration is formed and pulled out. This defect reaction can be followed up in the DCD plot given in figure 6. The patterns of the moving and resting defects before and after interaction are shown. The resulting defect complex (d + e) shows enhanced CL contrast resulting obviously from a superposition of contrast contributions of the individual defects (d) and (e). The pulled-out defect structure (s) is believed to constitute two parallel screw-type line segments. Its contrast behaviour is reflected by the slightly darker area in between the patterns (d + e) and (s).

Revealing the mobile dislocations as recombination centres by means of Dyn CL microscopy proves their intrinsic electronic properties. Distinct type-dependent recombination behaviour may be expected to be recognizable at separate dislocation segments exhibiting screw- and edge-type structures. The CL micrograph in figure 7 contains among others the CL contrasts of dislocation half-loops (s–e–s) expanding preferably in the $\langle 11\bar{2}0 \rangle$ crystallographic direction of the arm of a dislocation rosette investigated on the (0001) surface of a ZnO sample.

Asymmetric expansion of the loop structures hints at different mobilities for the edge- and screw-type dislocation segments. The faster loop parts may be identified as the edge-type segments having B(g) character as can be deduced from the polar termination of the (0001) sample surface. The edge-type segments obviously exhibit stronger CL contrasts if compared with the contrast values observed at the screw line segments.

The behaviour of CL contrasts at the screw- and edge-type dislocation segments seems to be indicative of differences in the recombination activity; however, reliable measurements of a

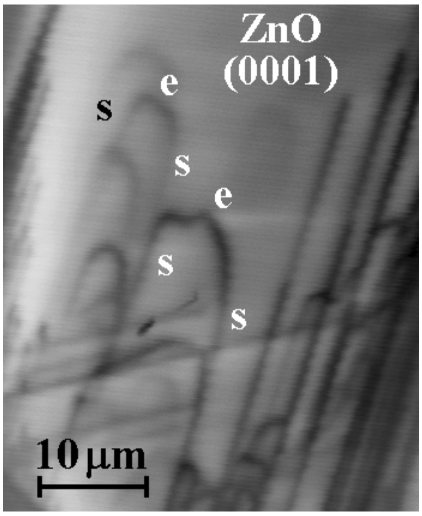

Figure 7. CL micrograph showing propagation of dislocation half-loops (s–e–s) expanding preferably in the $\langle 11\bar{2}0\rangle$ direction by basal plane slip. (e) and (s) label edge- and screw-type segments respectively. Stronger CL contrast for edge-type parts is clearly seen.

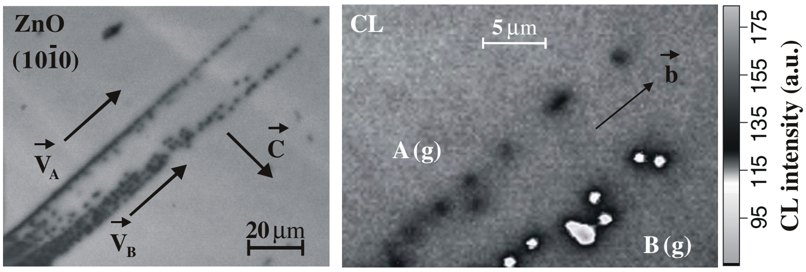

Figure 8. CL picture (a) illustrates the movement of threading edge-type dislocation segments with polar A(g) and B(g) core structure, respectively, which occur in the same arm of a dislocation rosette generated by indentation on a $(10\bar{1}0)$ ZnO sample surface. CL map (b) created by means of a special grey scale contrast mode shows the different strength of the single defect CL contrast in the A(g) and B(g) branch.

true contrast ratio are only possible if both segments acquired belong to an identical dislocation half-loop which must expand in a surface-parallel glide plane as realized in the present case. A characteristic contrast ratio of about 1.4–1.6 is found by CL profile analyses.

Dislocations with polar A(g) or B(g) core structures determined by A- or B-atom termination of the extra half planes occur side by side in the dislocation rosettes of indentations on $(10\bar{1}0)$ sample surfaces. Figure 8 is the CL picture of a relevant rosette arm pointing in the $\langle 11\bar{2}0\rangle$ direction.

According to the orientation of the *c*-axis, threading segments of the A(g) and B(g) dislocations are collocated in the two parallel branches formed in the rosette arm. Clearly different slip velocities for the A(g) and B(g) dislocations are evidenced by means of the CL movies taken during *in situ* indentation experiments. The ratio between the velocities measured for the opposite polar threading segments amounts to:

$$V_B/V_A = 10.$$

The given dislocation arrangement allows a detailed investigation of the CL contrast strengths appearing at the A(g) and B(g) dislocation segments. Figure 8(b) shows the CL map displaying a different CL contrast intensity at single defects belonging to the A(g) and B(g) group respectively. Evaluation of the CL contrast values at the threading segments of the individual dislocations yields:

$$C_A/C_B \approx 0.7.$$

Thus, higher recombination activity corresponding to higher defect mobility can be established for the polar B(g)-type dislocations in ZnO.

4. Conclusion

The dynamic mode of SEM CL is introduced as a very suitable technique for studying the dynamics of glide dislocations on a microscopic scale in direct relationship to the recombination properties of individual single defects being in the moving or resting state. The Dyn CL experiments disclose dislocations gliding at 'low temperature' under conditions of thermally activated or REDG-induced slip in GaAs and ZnO respectively, as extended mobile recombination centres. A non-radiative recombination activity appears immediately after generating the dislocations. No striking impact of dislocation slip movement on the efficiency of the defect-bound carrier recombination process is found.

Some interesting peculiarities of the microscopic dislocation dynamics are considered. In same local area of a strain gradient neighbouring dislocations are shown to exhibit accelerated and decelerated motion or antiparallel slip hinting at type-dependent mobilities. There are also contemporaneous processes of formation and back formation of dislocation segments. Furthermore, the defect reaction observed between a resting dislocation and a mobile one is found to affect the dynamic dislocation behaviour and defect-bound CL contrasts as well.

In GaAs representing the compound semiconductor with zincblende structure, the glide dislocations clearly exhibit type-dependent dynamics, but similar non-radiative recombination activity must be stated for the screw dislocations and for the 30°, 60° or 90° dislocation segments as well. No influence of the polar core structure in the edge-type dislocations on the recombination activity can be recognized.

The freshly produced glide dislocations in the ZnO samples with wurtzite lattice structure are seen to be very efficient carrier recombination centres. The recombination strength of the edge-type dislocation segments proves higher than that of the screw-type line segments.

It is worth mentioning that the polar A(g) and B(g) dislocations appearing in the wurtzite structure of ZnO have distinct recombination activity and show remarkable differences in their dynamic properties. The B(g)-type dislocation segments possess the higher recombination efficiency corresponding to higher dynamic mobility as compared with the behaviour of the A(g) dislocation segments.

Acknowledgments

The authors thank D M Hofmann, Universitaet Giessen, for supplying ZnO samples. Special thanks is due to Dipl.-Eng. Hermann Maehl for technical support.

Part of this work was performed in the framework of the 'Graduiertenkolleg 415' der Deutschen Forschungsgemeinschaft.

References

[1] Yacobi B G and Holt D B 1990 *Cathodoluminescence Microscopy of Inorganic Solids* (New York: Plenum) p 125
[2] Schreiber J and Hergert W 1989 *Inst. Phys. Conf. Ser.* **104** 97
[3] Hoering L 2001 *Thesis* Universitaet Halle
[4] S Vasnyov and Schreiber J 2003 *J. Phys.: Condens. Matter* **16** S269
[5] Schreiber J 1977 *Thesis* Universitaet Halle
[6] Hoering L 1998 *Diploma Work* Universitaet Halle
[7] Gottschalk H 1983 *J. Physique Coll.* **44** C4 475
[8] Rebane Yu T and Shreter Yu G 1991 *Springer Proc. Phys.* vol 54, ed J H Werner and H D Strunk (Berlin: Springer) p 28
[9] Maeda K and Takeuchi S 1996 *Dislocations in Solids* vol 10, ed F R N Nabarro and M S Duesbery (Amsterdam: North-Holland) p 445
[10] Holt D B 1962 *J. Phys. Chem. Solids* **23** 1353–62
[11] Osipyan Yu A and Smirnova I S 1968 *Phys. Status Solidi* **30** 19
[12] Hoering L, Schreiber J and Hilpert U 2001 *Solid State Phenom.* **78/79** 143
[13] Maeda K and Takeuchi S 1983 *J. Physique Coll.* **44** C4 375
[14] Maeda K, Suzuki K, Yamashita Y and Mera Y 2000 *J. Phys.: Condens. Matter* **12** 10079–91